

Extreme events in near integrable lattices

C. Hoffmann,^{1,2} E. G. Charalampidis,¹ D. J. Frantzeskakis,³ and P. G. Kevrekidis¹

¹*Department of Mathematics and Statistics, University of Massachusetts Amherst, Amherst, MA 01003-4515, USA*

²*Institut für Physik, Universität Oldenburg, D-26111 Oldenburg, Germany*

³*Department of Physics, National and Kapodistrian University of Athens, Panepistimiopolis, Zografos, Athens 15784, Greece*

(Dated: April 6, 2024)

In the present work, we examine the potential robustness of extreme wave events associated with large amplitude fluctuations of the Peregrine soliton type, upon departure from the integrable analogue of the discrete nonlinear Schrödinger (DNLS) equation, namely the Ablowitz-Ladik (AL) model. Our model of choice will be the so-called Salerno model, which interpolates between the AL and the DNLS models. We find that rogue wave events essentially are drastically distorted even for very slight perturbations of the homotopic parameter connecting the two models off of the integrable limit. Our results suggest that the Peregrine soliton structure is a rather sensitive feature of the integrable limit, which may not persist under “generic” perturbations of the limiting integrable case.

PACS numbers:

I. INTRODUCTION

The study of phenomena associated with extreme events and rogue waves has gained substantial traction over the last few years [1–4]. This can largely be attributed to the development of experimental settings in a variety of fields where the relevant coherent structures can be systematically created and observed. These fields range from superfluid helium [5] to hydrodynamics [6–8], and from nonlinear optics [9–14] and plasmas [15] to Faraday surface ripples [16] and parametrically driven capillary waves [17]. Experimental efforts have, in part, been motivated by – and also inspired – numerous theoretical investigations, mainly concerning variants of the nonlinear Schrödinger (NLS) equation. The theoretical activity has now been summarized in numerous reviews [18–20], as well as books [1–4].

One of the significant aspects of the investigation of extreme wave events has to do with the structural form that these events assume, and perhaps especially with their robustness in NLS and related models. The seminal works of Peregrine [21], Kuznetsov [22], Ma [23], and Akhmediev [24], as well as of Dysthe and Trulsen [25], have provided a framework of study of relevant coherent structures, either periodic in space (such as the Akhmediev breather) or periodic in time (such as the Kuznetsov-Ma breather) or, most notably, localized in space-time, as the Peregrine soliton [21]. A question then emerges about whether these entities survive model perturbations and/or emerge under generic classes of initial conditions. Admittedly, the latter question has only been partially addressed. For instance, in a class of perturbations involving Hirota-model variants (such as third-order dispersion and self-steepening terms), a perturbed, still algebraically decaying variant of the Peregrine soliton was obtained (however its persistence was not ensured to all orders in the perturbation) [26]. Moreover, adiabatic approximations [27] and perturbed inverse scattering approaches [28] have considered the stability of Kuznetsov-Ma (KM) solitons indicating their potential robustness against dispersive but non-robustness against dissipative perturbations. A different perspective on the emergence of localized phenomena in space-time was given by the work of [29], where it was argued that the proximity of such solutions to chaotic states (in more elaborate, non-integrable models) appears to increase the occurrence of extreme events. Other works have focused on the stability properties of solutions [30–32]; however, there is an ambiguity associated with the time-dependent nature of the solutions. A natural setup for performing stability studies is, arguably, the Floquet analysis of the time-periodic KM solution [33].

In a recent work [34], a different type of “genericity” of these solutions was considered: the emergence of extreme events stemming from simple –yet typical– Gaussian initial data, under a phenomenon called gradient catastrophe that has been explained in the pioneering work of [35]. In particular, it was proposed that in the semiclassical limit of the NLS model, such initial data will lead to the formation of an array of essentially identical (up to small corrections) Peregrine soliton-like structures, which emerge at the poles of the so-called tritronquée solution of the Painlevé I equation. The importance of these findings is underscored by the fact that very recently the universality of this emergence of the Peregrine soliton in the semiclassical focusing dynamics of the NLS model has been manifested experimentally [36]. Furthermore, recently such Peregrine waveforms were also found to spontaneously emerge as a result of the interaction of dispersive shock waves in [37].

Our aim in the present work is to explore the relevance of Peregrine-soliton type solutions in spatially discrete systems, i.e., in nonlinear dynamical lattices. There has been an amount of work in this context as well. In particular, it has been established that a Peregrine-like solution, strongly reminiscent of its continuum sibling exists [38] in

the context of the completely integrable discrete version of the NLS equation, the so-called Ablowitz-Ladik (AL) model [39, 40]. In fact, subsequent work has established the systematic construction of higher-order such solutions [41]. However, it is also well-known that while the AL model is useful for the consideration of numerous perturbative calculations involving single discrete solitons [42], their stability [43] and their collisional dynamics [44], it is not of direct relevance to experimental settings. On the contrary, the quintessential discrete model of relevance, both to nonlinear optics (in the context of arrays of coupled waveguides) and to atomic Bose-Einstein condensates (BECs) confined in optical lattices, is the discrete nonlinear Schrödinger (DNLS) equation [45]. Hence, our considerations herein will involve departing in a systematic way from the AL model and approaching the DNLS one. This will be done through the Salerno model [46], interpolating between the two limits.

We consider a Gaussian initial profile (as a generic waveform) and examine a two-parametric variation. In particular, on the side of varying the initial condition parameters, we examine the effect of changing the variance of the initial condition (IC). Here, using a large variance places us within the so-called semi-classical regime [35], where we may expect analogously to the continuum case of [34] to observe Peregrine soliton like structures. On the other hand, at the level of varying the model, we consider changes of a homotopic parameter as extending from the AL limit all the way to the DNLS one, and examine a wide variety of cases in between. Our main observation is that at the AL limit, we identify Peregrine structures and even a space-time evolution featuring the emergence of a “Christmas-tree”-like pattern, analogous to the continuum case [34], as an apparent discrete emulation of the gradient catastrophe phenomenology of [35]. Nevertheless, this appears to be—in some sense—a singular case, in that as soon as we depart from this integrable limit, the prevalent dynamical structures appear to consist of persistent or breathing in time discrete solitonic entities (discussed at length in the context of DNLS models [45]), rather than of Peregrine-like patterns. It is intriguing to point out that a similar conclusion (a propensity towards freak waves near the integrable limit) had emerged through the important statistical analysis of Ref. [47]. In fact, our observations lead us to conjecture that no direct analogue of the Peregrine soliton exists in the DNLS model, although one exists in its continuum limit, as well as in its integrable discrete sibling. A dynamical systems analysis that would tackle this persistence problem would be of paramount importance for future work.

Our presentation is structured as follows. In section II, we present the relevant mathematical model(s) and the corresponding prototypical solutions. In section III, we establish the corresponding numerical results and comment on the relevant observations. Finally, in section IV, we present a summary of our findings and provide some suggestions for future work.

II. THE MODEL

The model of interest originates from the focusing NLS equation, written in dimensionless form as follows:

$$i\partial_t u = -\frac{1}{2}\partial_x^2 u - |u|^2 u, \quad (1)$$

where $u(x, t) \in \mathbb{C}$ is the wave function. Next, discrete realizations of Eq. (1) can be obtained, e.g., by replacing the (continuous) dependent variable $u(x, t)$ with $u_n(t) \doteq u(x_n, t)$ ($x_n = -L + nh$ with L the grid’s half-width) and the second partial derivative with its central finite difference operator. This way, we obtain the discrete NLS (DNLS) equation:

$$i\dot{u}_n = -\frac{1}{2h^2}(u_{n+1} - 2u_n + u_{n-1}) - |u_n|^2 u_n, \quad n \in \mathbb{Z}, \quad (2)$$

where overdot stands for differentiation with respect to time and, hereafter, we will set the lattice spacing $h = 1$. Details on the derivation and physical origin of the DNLS, e.g., in coupled optical waveguides and in BECs confined in optical lattices, as well its discrete soliton solutions, can be found in the review [45].

A different discretization of Eq. (1) can be obtained by discretizing the field value multiplying the square modulus in Eq. (2) as $u_n \doteq (u_{n+1} + u_{n-1})/2$. The resulting discrete lattice model is the AL model [39, 40], which is of the form:

$$i\dot{u}_n = -\frac{1}{2}(u_{n+1} - 2u_n + u_{n-1}) - \frac{1}{2}|u_n|^2(u_{n+1} + u_{n-1}). \quad (3)$$

To interpolate between the DNLS and the AL models, we introduce a real parameter $\mu \in [0, 1]$. Then, we can write the following “tunable” discrete lattice system:

$$i\dot{u}_n = -\frac{1}{2}(u_{n+1} - 2u_n + u_{n-1}) - \mu|u_n|^2 u_n - \frac{1}{2}(1 - \mu)|u_n|^2(u_{n+1} + u_{n-1}), \quad (4)$$

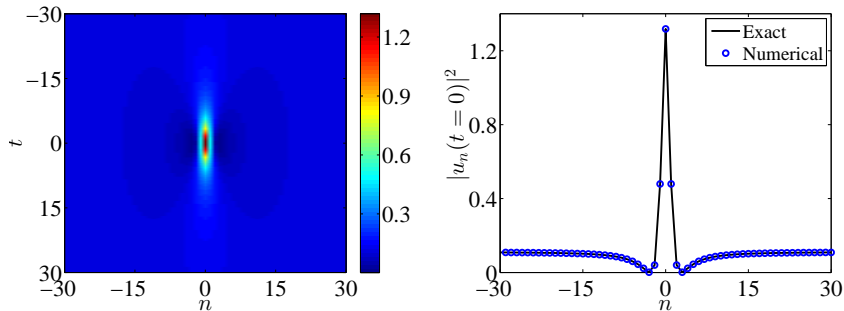


FIG. 1: (Color online) Numerical results for the Ablowitz-Ladik (AL) model with Peregrine soliton initial data, given by Eq. (5). The spatiotemporal evolution of the density $|u_n|^2$ is shown in the left panel, whereas the spatial distribution of the density evaluated at $t = 0$ is presented in the right panel, with blue open circles; the exact solution is plotted too, with a black solid line, for comparison.

which corresponds to the DNLS and AL models for $\mu = 1$ and $\mu = 0$, respectively. This generalized Salerno model [46] of Eq. (3) will be the focal point of our subsequent numerical investigations.

Here, it should be noted that the AL model supports rational solutions of the rogue wave type: in particular, the first-order such rational solution of the AL system is of the form [38]:

$$u_n = U_n e^{i\phi}, \quad U_n(t) = \left(\frac{4q(1+q^2)(1+2iq^2t)}{1+4q^2n^2+4q^4(1+q^2)t^2} - q \right) e^{iq^2t}, \quad (5)$$

with q and ϕ being a real background amplitude and (arbitrary) phase, respectively. It is to that solution that we will compare our findings, especially so in computations associated with the AL limit. In that light, the background amplitude q will be utilized as a fitting parameter to obtain the “best-fit” Peregrine soliton.

Our goal is to study the initial value problem (IVP) which consists of Eq. (4) (for various values of $\mu \in [0, 1]$) and Gaussian initial data, of the form:

$$u_n(t=0) = e^{-n^2/2\sigma^2}, \quad (6)$$

where σ characterizes the Gaussian’s width. In a vein reminiscent of the work of [34], we are interested in identifying parametric regimes of both σ and μ , such that extreme events (or fundamental solitons) at the discrete level can be obtained.

III. NUMERICAL RESULTS

Our exposition of numerical results commences with the case of Eq. (4) for $\mu = 0$, i.e., the AL model. Specifically, periodic boundary conditions are employed on a lattice containing $N = 512$ points. At first, and as a benchmark case, we initialize the dynamics with the Peregrine soliton given by Eq. (5) at $t = -30$, with $q = 1/3$ and $\phi = 0$; the results are presented in Fig. 1. It can be discerned from this figure that the formation of the Peregrine soliton is clearly evident (see the left panel therein), as well as that the numerics compare well with the exact results (see the right panel of the same figure, where densities at $t = 0$ of the exact and numerical solutions are presented).

Next, and still in the realm of the AL model, we initialize the dynamics using the discrete Gaussian wavepacket given by Eq. (6). Representative results with $\sigma = 30$ and $\sigma = 15$ are presented in the top and bottom rows of Fig. 2, respectively. For large values of the Gaussian’s width, extreme events can be seen to form (see also Ref. [34] for the continuum NLS case) in a way strongly reminiscent of the Peregrine solitons at the discrete level (see the right panels of Fig. 2). Some observations are in order here. On the one hand, it appears evident that gradient catastrophe type phenomena are still present in the discrete case, in analogy with the continuum one [35]. Moreover, extreme intensities are achieved due to the ability of the discrete problem to collect a large fraction of the original mass at a single site (in the continuum 1D problem, the mass conservation and absence of collapse do not favor such an extreme accumulation). The individual constituents of the resulting structure, much reminiscent of the “Christmas tree” pattern of Ref. [34] are evidently well approximated by a Peregrine soliton. As shown in the right panel near the core, a Peregrine pattern of the same maximal intensity allows to closely approximate the core of the wave, although

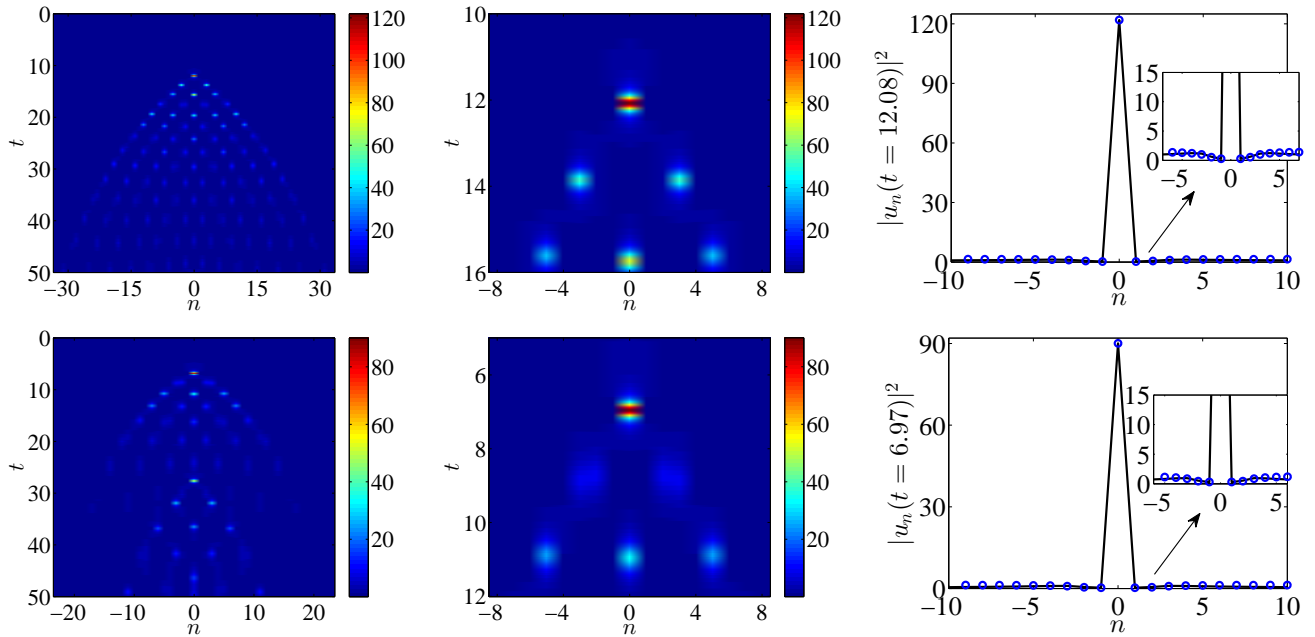


FIG. 2: (Color online) Numerical results for the Ablowitz-Ladik (AL) model [cf. Eq. (4) for $\mu = 0$] with Gaussian initial data for $\sigma = 30$ (top row) and $\sigma = 15$ (bottom row). The left column shows the spatiotemporal evolution of the density $|u_n|^2$ while its zoom-in is presented in the middle column for the respective cases. Spatial distribution of the density at $t = 12.08$ and $t = 6.97$ (i.e., when the first peak is formed) is depicted by blue open circles in the right column. The Peregrine solution with the same maximal amplitude according to Eq. (5) is depicted by solid black lines in the right column as well.

obviously the different asymptotics of the Gaussian vs. the exact Peregrine necessitate a deviation between the two far enough from the center. Lastly, other things partially differ from the generic continuum picture drawn through the insights of Ref. [35]. For instance, the discrete nature of space (not allowing the solitons to be centered exactly at the poles of the tritonquée solutions) leads to a substantial variation of amplitude between the different peaks.

We now consider deviations of the AL model, so that we can examine whether those features remain present as we approach the more physically relevant DNLS limit. Results for a small finite value of μ (i.e., close to the AL limit), namely for $\mu = 0.05$, are presented in the top row of Fig. 3. Already here, it can be seen that while the phenomenology of features associated with a gradient catastrophe is still present, the structure is not as closely connected to the Peregrine (it rapidly deviates from it). This may be attributed to the fact that we only know the exact Peregrine soliton solution analytically in the AL case. Nevertheless, a more striking feature arises near $n = 0$ in the top panel, and more drastically so throughout the evolution in the bottom panel, where $\mu = 0.8$ (i.e., closer to the DNLS limit). This has to do with the emergence of persistent breathing patterns, which can be associated with discrete solitons (or discrete breathers) of the DNLS model. These have a fundamental difference in their phenomenology in comparison with the Peregrine in that while they are localized in space, they are no longer localized also in time (the latter is a crucial feature for waves that “appear out of nowhere and disappear without a trace” [48]). It is important that such breathing, persistent features emerge not only for the large μ values of the bottom panel (where one can argue that we are rather far away from integrability), but also even at rather small values such as $\mu = 0.05$ of the top panel. To further test this, we have conducted simulations at smaller values of μ (down to $\mu = 0.01$), confirming that similar features do arise. In that sense, it seems more appropriate to argue—in line also with the observations of [47]—that the integrable limit is special and, in a sense, seemingly rather singular as regards the persistence of rogue wave structures. Nevertheless, this is not a proof, and there may well be perturbations for which the structure survives. This topic certainly merits further investigation.

We now consider the other end/limit, and study the special DNLS case of $\mu = 1$ for different values of σ ; pertinent results are shown in Fig. 4. Here, too, we can observe that the focusing process may have a gradient catastrophe character—see especially the top right panel of the figure—although the phenomenon seems less extreme in the middle and bottom right panels. Once again, we furthermore emphasize the apparent persistence of the structures that are emerging (notice the “threads” of the relevant patterns and their “breathing” in the left and middle panels). This implies that the relevant configurations are less structurally proximal to Peregrine solitons and more so to discrete solitonic structures.

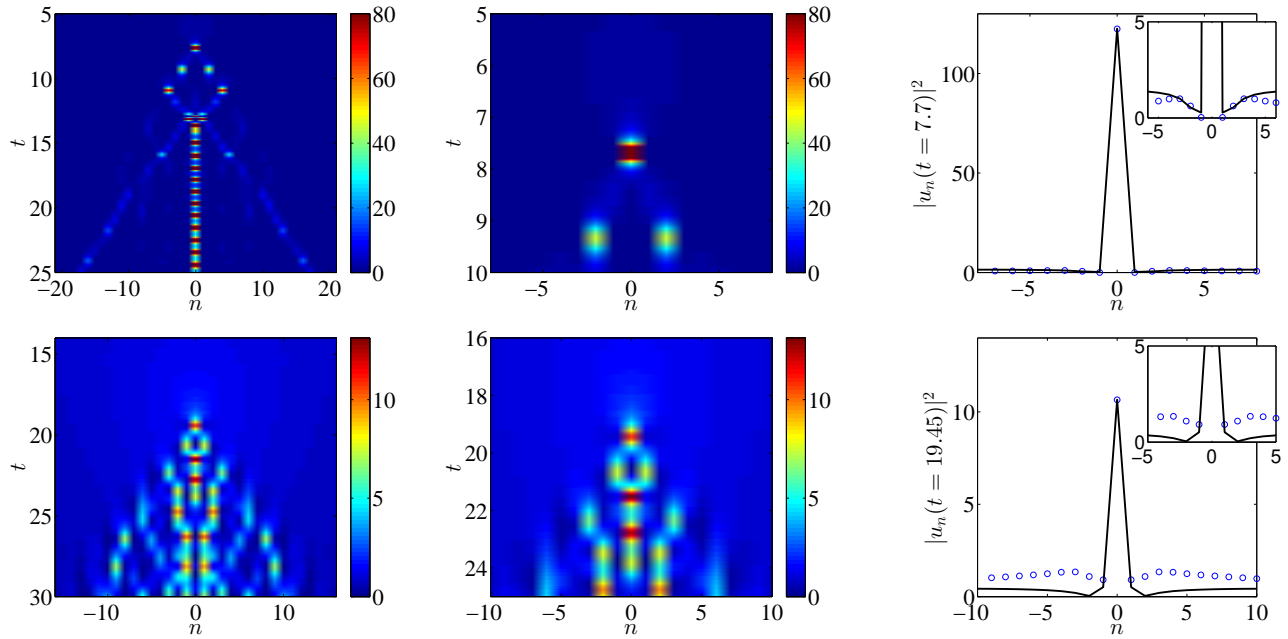


FIG. 3: (Color online) Numerical results for the Salerno model [cf. Eq. (4)] with Gaussian initial data for $\mu = 0.05$ and $\sigma = 3.3$ (top row) and for $\mu = 0.8$ and $\sigma = 7.4$ (bottom row). The left column shows the spatiotemporal evolution of the density $|u_n|^2$, while its zoom-in is presented in the middle column. The spatial distribution of the density at $t = 7.7$ and $t = 19.45$ (i.e., when the first peak is formed) is depicted by blue open circles in the right column. The best-fit Peregrine soliton solution, according to Eq. (5), is depicted by solid black lines in the right column as well. Notice the (progressively) deteriorating agreement between the two.

In a broader picture, the panels displayed in Fig. 5 provide an overview of those features. This figure is intended as an effective “two-parameter diagram” from the point of view of the dynamics of the Salerno model for initial conditions of different width, and different values of the parameter μ , ranging from the integrable to progressively more non-integrable cases (an animated figure showing the behaviour for $\sigma \in [0.1, 30]$ is available at [50]). The left column shows the integrable AL model as a reference. The middle column highlights a weak perturbation of the integrable limit for the case of $\mu = 0.02$ (available at [51]). Finally, a substantial departure from the integrable limit is displayed for $\mu = 0.5$ in the right column (available at [52]). All those are compared for specific values of σ in each row. In the topmost row, the case of small σ , i.e., $\sigma = 0.6$, illustrates a fairly similar behavior, irrespectively of the value of μ . A breathing dynamics appears to ensue (reminiscent of 2-soliton solutions; see the relevant discussion in Ref. [34]) and the only feature changing across the columns is the period of the relevant pattern.

The differences across the columns are starting to be more pronounced in the second row for the case of $\sigma = 1.2$. The left panel, as expected for the integrable scenario, develops a solitonic character of a multi-soliton state (cf. also the corresponding discussion of Ref. [34]). However, already at small departures from integrability a robust structure emerges near the center and is even more pronounced and permanent in the case of $\mu = 0.5$. These features are even further amplified in the third row featuring the case of $\sigma = 4.2$. Here the AL pattern clearly re-creates the Christmas-tree-type pattern that was observed in the corresponding continuum NLS model. Nevertheless, the non-integrable model even for a slight deviation, such as $\mu = 0.02$, changes the dynamics drastically and no longer enables the propagation of the dendritic structure. Instead, three filamentary breathing patterns appear to occur and survive as long-lived entities in the corresponding dynamics. This departure remains pronounced in the case of $\mu = 0.5$ in the right panel of the third row.

For even larger values of σ the tree structure, which started out in a triangular shape for the AL model (with the angle of the outer slope changing depending on σ), eventually changes to a parabolic shape with the extreme events packed closely together. A rather similar behaviour is shown for $\mu = 0.02$, while $\mu = 0.5$ is much more extreme, with some events apparently being able to linger on for quite some time.

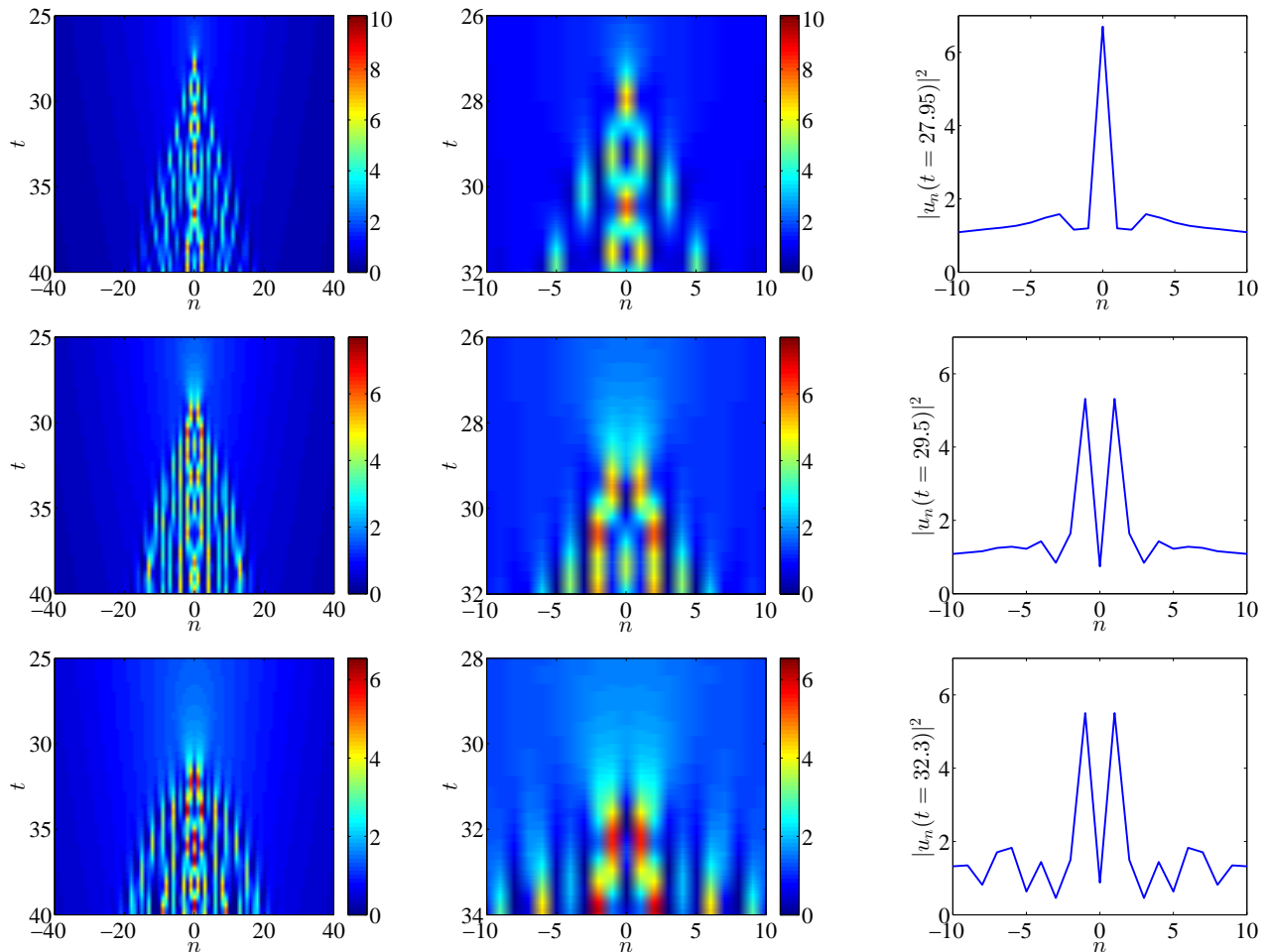


FIG. 4: (Color online) Numerical results for the Salerno model [cf. Eq. (4)] in the DNLS limit, i.e., for $\mu = 1$, with Gaussian initial data, with $\sigma = 9.6$ (top row), $\sigma = 9.8$ (center row) and $\sigma = 11$ (bottom row). The left column shows the spatiotemporal evolution of the density $|u_n|^2$ while its zoom-in is presented in the middle column. Spatial distribution of the density at $t = 27.95$ (top), $t = 29.5$ (center) and $t = 32.3$ (bottom) (i.e., when the first peak is formed) is depicted by solid blue lines in the right column.

IV. CONCLUSIONS AND FUTURE WORK

In the present work, we have investigated the formation of Peregrine soliton-like patterns in the far less studied nonlinear dynamical lattices, such as the Ablowitz-Ladik, the discrete nonlinear Schrödinger, as well as the Salerno model that interpolates between the two. In a similar class of models, and differently than the important statistics-based work of [47], we have based our investigation on the experience obtained from the continuum sibling of the model. This has been done in part due to using a (generic) Gaussian initial datum that was shown to give rise in the continuum, in the appropriate semi-classical regime, to Peregrine-type solitons [34]. Even more importantly, it has been based on the fundamental mathematical understanding of the emergence of the phenomenon of gradient catastrophes and the formation during the latter of Peregrine-like structures, as per the key work of [35].

Indeed, in the discrete integrable model too, relevant Peregrine structures (analytically known per the work of [38, 41]) were found to emerge as a result of the gradient catastrophe in the semi-classical regime, just like multi-soliton solutions were identified away from it. On the other hand though, it was found that even weak deviations from the integrable limit would substantially blur the picture, and appear to give rise to more permanent/persistent breathing patterns which seemed less consonant with the fundamental premise of “appearing out of nowhere and disappearing without a trace”.

In that light, a key question concerns whether (as we conjectured herein) it may be possible to prove that the Peregrine soliton, as a homoclinic solution in space-time, no longer persists as soon as the discrete, non-integrable

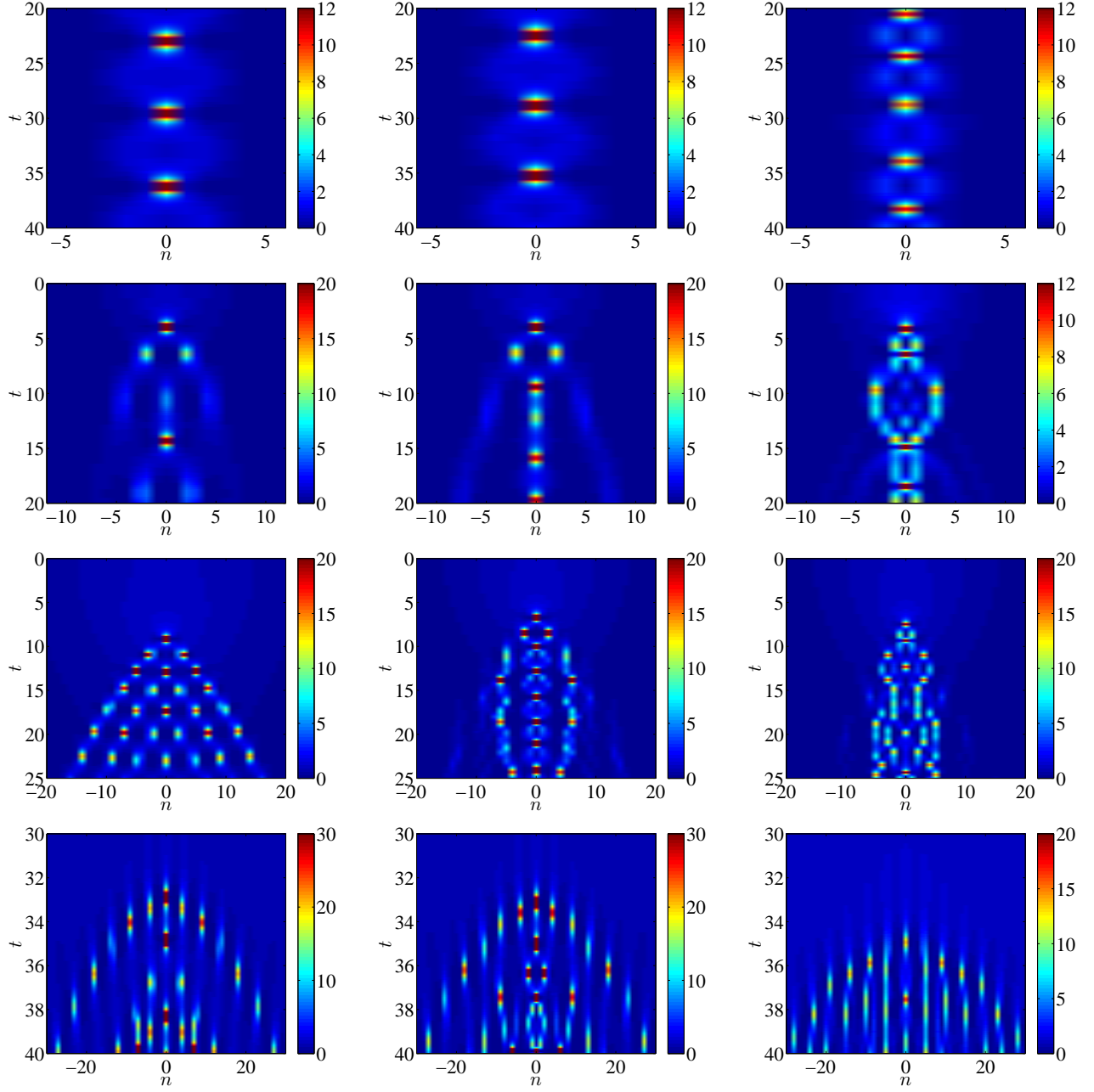


FIG. 5: (Color online) Numerical results for the Salerno model, Eq. (4), with Gaussian initial data, for $\mu = 0$ (left column, the AL model), $\mu = 0.02$ (center column, weak deviation from AL) and $\mu = 0.5$ (right column, halfway between AL and DNLS). The first row shows the spatiotemporal evolution of the density $|u_n|^2$ for $\sigma = 0.6$, the second for $\sigma = 1.2$, the third for $\sigma = 4.2$ and the last for $\sigma = 18.6$. Similarities (especially in the first and fourth rows) and differences (especially in the second and third rows) between the different settings are discussed in the text.

perturbation comes into play. Performing (perhaps) a Melnikov-type analysis and appreciating conditions enabling (or avoiding) the existence of Peregrine soliton like waveforms would seem to be an especially intriguing topic for future work. Another potentially interesting question might concern the relevance of Peregrine patterns for the dynamics of higher-dimensional models. For instance, the AL model in higher dimensions is known [49] (although it has received very limited attention) and moreover it possesses by construction the 1D (uniform in the second spatial variable) Peregrine solution. A question of interest concerns the “transverse robustness” of this Peregrine and the dynamical outcome of phenomena such as the gradient catastrophe in higher-dimensional settings. These features are presently

under study and will be reported in future publications.

Acknowledgments

P.G.K. and D.J.F. acknowledge that this work was made possible by NPRP Grant No. 8-764-1-160 from Qatar National Research Fund (a member of Qatar Foundation). C.H. and P.G.K. gratefully acknowledge that this work was made possible by support from FP7, MarieCurie Actions, People, International Research Staff Exchange Scheme (IRSES-606096). P.G.K. also acknowledges enlightening discussions with Profs. G. Tsironis and A. Tovbis on the subject.

-
- [1] E. Pelinovsky and C. Kharif (eds.), *Extreme Ocean Waves* (Springer, NY, 2008).
 - [2] C. Kharif, E. Pelinovsky, and A. Slunyaev, *Rogue Waves in the Ocean* (Springer, NY, 2009).
 - [3] A. R. Osborne, *Nonlinear Ocean Waves and the Inverse Scattering Transform* (Academic Press, Amsterdam, 2010).
 - [4] M. Onorato, S. Residori, and F. Baronio, *Rogue and Shock Waves in Nonlinear Dispersive Media*, Springer-Verlag (Heidelberg, 2016).
 - [5] A. N. Ganshin, V. B. Efimov, G. V. Kolmakov, L. P. Mezhov-Deglin, and P. V. E. McClintock, Phys. Rev. Lett. **101**, 065303 (2008).
 - [6] A. Chabchoub, N. P. Hoffmann, and N. Akhmediev, Phys. Rev. Lett. **106**, 204502 (2011).
 - [7] A. Chabchoub, N. Hoffmann, M. Onorato, and N. Akhmediev, Phys. Rev. X **2**, 011015 (2012).
 - [8] A. Chabchoub and M. Fink, Phys. Rev. Lett. **112**, 124101 (2014).
 - [9] D. R. Solli, C. Ropers, P. Koonath, and B. Jalali, Nature **450**, 1054 (2007).
 - [10] B. Kibler *et al.*, Nature Phys. **6**, 790 (2010).
 - [11] B. Kibler *et al.*, Sci. Rep. **2**, 463 (2012).
 - [12] J. M. Dudley, F. Dias, M. Erkintalo, and G. Genty, Nat. Photon. **8**, 755 (2014).
 - [13] B. Frisquet *et al.*, Sci. Rep. **6**, 20785 (2016).
 - [14] C. Lecaplain, Ph. Grelu, J. M. Soto-Crespo, and N. Akhmediev, Phys. Rev. Lett. **108**, 233901 (2012).
 - [15] H. Bailung, S. K. Sharma, and Y. Nakamura, Phys. Rev. Lett. **107**, 255005 (2011).
 - [16] H. Xia, T. Maimbourg, H. Punzmann, and M. Shats, Phys. Rev. Lett. **109**, 114502 (2012).
 - [17] M. Shats, H. Punzmann, and H. Xia, Phys. Rev. Lett. **104**, 104503 (2010).
 - [18] Z. Yan, J. Phys. Conf. Ser. **400**, 012084 (2012).
 - [19] P. T. S. DeVore, D. R. Solli, D. Borlaug, C. Ropers, and B. Jalali, J. Opt. **15**, 0640031 (2013).
 - [20] M. Onorato, S. Residori, U. Bortolozzo, A. Montinad, and F. T. Arecchi, Phys. Rep. **528**, 47 (2013).
 - [21] D. H. Peregrine, J. Austral. Math. Soc. B **25**, 16 (1983).
 - [22] E. A. Kuznetsov, Sov. Phys.-Dokl. **22**, 507 (1977).
 - [23] Ya. C. Ma, Stud. Appl. Math. **60**, 43 (1979).
 - [24] N. N. Akhmediev, V. M. Eleonskii, and N. E. Kulagin, Theor. Math. Phys. **72**, 809 (1987).
 - [25] K. B. Dysthe and K. Trulsen, Phys. Scr. **T82**, 48 (1999).
 - [26] A. Ankiewicz, N. Devine, and N. Akhmediev, Phys. Lett. A **373**, 3997 (2009).
 - [27] L. Gagnon, J. Opt. Soc. Am. B **10**, 469 (1993).
 - [28] J. Garnier and K. Kalimeris, J. Phys. A: Math. Theor. **45**, 035202 (2012).
 - [29] A. Calini and C. M. Schober, pp. 31–51 in Ref. [1].
 - [30] R. A. Van Gorder, J. Phys. Soc. Jpn. **83**, 054005 (2014).
 - [31] U. Al Khawaja, H. Bahlouli, M. Asad-uz-zaman, and S.M. Al-Marzoug, Commun. Nonlinear Sci. Numer. Simulat. **19**, 2706 (2014).
 - [32] U. Al Khawaja, S.M. Al-Marzoug, H. Bahlouli, and M. Asad-uz-zaman, Commun. Nonlinear Sci. Numer. Simulat. **32**, 1 (2016).
 - [33] J. Cuevas-Maraver, P. G. Kevrekidis, D. J. Frantzeskakis, N. I. Karachalios, M. Haragus, and G. James Phys. Rev. E **96**, 012202 (2017).
 - [34] E. G. Charalampidis, J. Cuevas-Maraver, D. J. Frantzeskakis, and P. G. Kevrekidis, *Rogue waves in ultracold bosonic seas*, arXiv:1609.01798.
 - [35] M. Bertola and A. Tovbis, Comm. Pure Appl. Math. **66**, 678 (2013).
 - [36] A. Tikan, C. Billet, G. El, A. Tovbis, M. Bertola, T. Sylvestre, F. Gustave, S. Randoux, G. Genty, P. Suret, and J.M. Dudley Phys. Rev. Lett. **119**, 033901 (2017).
 - [37] G. El, E.G. Khamis, A. Tovbis, Nonlinearity **29**, 2798 (2016).
 - [38] A. Ankiewicz, N. Akhmediev, and J.M. Soto-Crespo, Phys. Rev. E **82**, 026602 (2010).
 - [39] M.J. Ablowitz and J.F. Ladik, J. Math. Phys. **16**, 598 (1975).
 - [40] M.J. Ablowitz and J.F. Ladik, J. Math. Phys. **17**, 1011 (1976).
 - [41] Y. Ohta and J. Yang, J. Phys. A **47**, 255201 (2014).

- [42] D. Cai, A.R. Bishop and N. Gronbech-Jensen, Phys. Rev. E **53**, 4131 (1996).
- [43] T. Kapitula and P. Kevrekidis, Nonlinearity **14**, 533 (2001).
- [44] S.V. Dmitriev, P.G. Kevrekidis, B.A. Malomed, and D.J. Frantzeskakis, Phys. Rev. E **68**, 056603 (2003).
- [45] P. G. Kevrekidis, *The Discrete Nonlinear Schrödinger Equation* (Springer, Berlin Heidelberg, 2009).
- [46] M. Salerno, Phys. Rev. A **46**, 6856 (1992).
- [47] A. Maluckov, Lj. Hadzievski, N. Lazarides, and G. P. Tsironis Phys. Rev. E **79**, 025601(R) (2009)
- [48] N. Akhmediev, A. Ankiewicz, and M. Taki, Phys. Lett. A **373**, 675 (2009).
- [49] P.G. Kevrekidis, G.J. Herring, S. Lafortune, and Q.E. Hoq, Phys. Lett. A **376**, 982 (2012).
- [50] <https://youtu.be/-X2XuU4o9RA>
- [51] <https://youtu.be/BvAg-H31k6o>
- [52] <https://youtu.be/WLW5uBVDCQI>

